Bioconjugate Chemistry

Article

pubs.acs.org/bc

Identification of Highly Reactive Cysteine Residues at Less Exposed Positions in the Fab Constant Region for Site-Specific Conjugation

Yasuhisa Shiraishi,* Takashige Muramoto, Kazutaka Nagatomo, Daisuke Shinmi, Emiko Honma, Kazuhiro Masuda, and Motoo Yamasaki

Innovative Technology Laboratories, Research Functions Unit, R&D Division, Kyowa Hakko Kirin Co., Ltd., Tokyo 194-8533, Japan

Supporting Information

ABSTRACT: Engineered cysteine residues are currently used for the site-specific conjugation of antibody−drug conjugates (ADC). In general, positions on the protein surface have been selected for substituting a cysteine as a conjugation site; however, less exposed positions (with less than 20% of accessible surface area [ASA]) have not yet been evaluated. In this study, we engineered original cysteine positional variants of a Fab fragment, with less than 20% of ASA, and evaluated their thiol reactivities through conjugation with various kinds of payloads. As a result, we have identified three original cysteine positional variants (heavy chain: Hc-A140C, light chain: Lc-Q124C and Lc-L201C), which exhibited similar monomer content, thermal stability, and antigen binding affinity in comparison to the wild-type Fab. In addition, the presence of cysteine in these positions made it possible for the Fab variants to react with variable-sized molecules with high efficiency. The favorable physical properties of the cysteine positional variants selected in our study suggest that less exposed positions, with less than 20% of ASA, provide an alternative for creating conjugation sites.

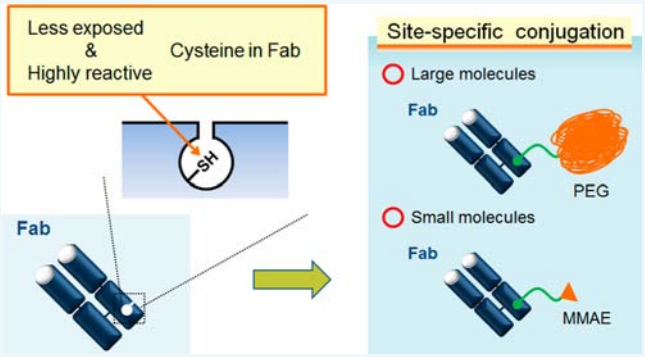

INTRODUCTION

Antibody−drug conjugates (ADCs) are a new class of highly potent drug formulations designed as a targeted therapy for the treatment of cancer patients. Targeted delivery of a cytotoxic drug to the tumor tissue leads to potential reduction in its toxicity toward healthy cells, and thus expands the therapeutic window. ADCs have shown significant progress in the clinical studies and the FDA has recently approved two such drugs, ado-trastuzumab emtansine (Kadcyla) and brentuximab vedotin (Adcetris). Furthermore, there are more than 30 ADC drugs in the pipeline that are currently undergoing clinical studies.[1]

The antibody conjugation methods currently used for the production of ADCs generally include a chemical reaction of the lysine ε-amino groups or the cysteine sulfhydryl groups, produced by reducing the interchain disulfide bonds.[2] These chemical techniques make it difficult to control the site-specificity and stoichiochemistry, which leads to the production of heterogeneous products. For instance, as determined by the peptide mapping, lysine conjugation results in 0−8 drug-to-antibody ratios (DAR), and about 40 different lysine residues per antibody are conjugated.[3] Hamblett et al. have reported that drug loading plays a dominant role in the pharmacokinetics, efficacy, and therapeutic index of the resulting ADC.[4] Specifically, the ADCs with higher DARs were found to be cleared faster and exhibited lower in vivo efficacy in comparison to those with lower DARs.

One way to overcome these challenges is through the use of site-specific conjugation, a technique in which a known number of linker-drug molecules are consistently conjugated to defined sites.[5,6] Currently, three cutting-edge strategies are available: insertion of the cysteine residues in the antibody sequence,[7−11] insertion of an unnatural amino acid with bio-orthogonal reactivity,[12,13] and enzymatic conjugation.[14,15] The engineering of antibodies with cysteine residues offers a particularly convenient method, as no cell line engineering and additional reagents are required. On the other hand, engineered free cysteine residues present on the surface of a protein could pair with cysteine residues present on other protein molecules, resulting in dimers.[16] It is also possible that the introduced cysteines could pair with the native cysteine residues in the same protein, resulting in protein misfolding.

Earlier studies had explored the surface positions on recombinant antibodies for the introduction of cysteine residues.[9] Junutula et al. reported new engineered cysteine residues (THIOMAB), which had moderate fractional surface area and were identified by unique phage display techniques (PHESELECTOR).[7] THIOMAB−drug conjugates displayed minimal heterogeneity with similar in vivo activity, improved pharmacokinetics, and a superior therapeutic index in

Received: February 6, 2015
Revised: May 10, 2015
Published: May 15, 2015

DOI: 10.1021/acs.bioconjchem.5b00080
Bioconjugate Chem. 2015, 26, 1032−1040

Scheme 1. Conjugation with Various Kind of Payloads

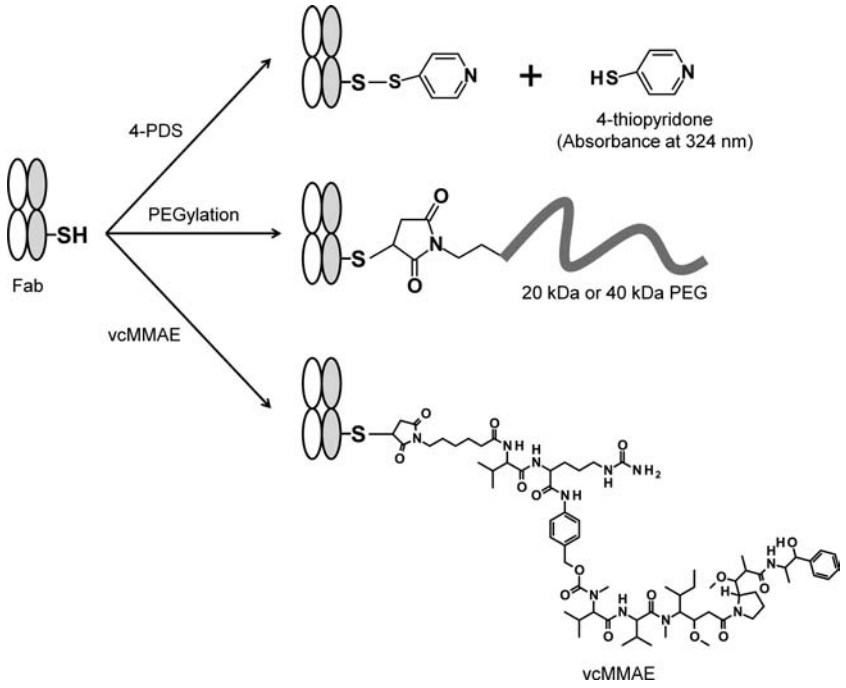

comparison to the conventional, randomly conjugated ADCs.[8] Further, Trout et al. reported the implementation of the spatial-aggregation propensity in order to identify the engineered cysteine residues with low aggregation and no structural abnormalities.[11]

Conjugation with functional molecules using cysteine at inaccessible positions is generally considered improper. For example, granulocyte-colony stimulating factor has a free cysteine residue at the less exposed position, which results in reduced PEGylation under physiological conditions.[17] Thus, owing to the above-mentioned factors, until now the approach for engineering cysteine has been confined to the positions with high and moderate accessible surface area (ASA). For the first time, in this study we have conducted an investigation of engineered cysteine residues at less exposed positions (with less than 20% of ASA) of the Fab constant region in order to expand the strategy for site-specific conjugation via engineered cysteines. In addition, we evaluated the binding capacity for macromolecules such as PEG, in order to apply our methodology to various-sized payloads (Scheme 1).

RESULTS

Selection Strategy for Cysteine Positions. In this study, trastuzumab was used as a model antibody for selecting the cysteine positions. Among the positions in the Fab constant region with less than 20% of ASA, 26 positions (Hc: 12 positions, Lc: 14 positions) were selected for the study, which were depicted onto the structure of Tra-Fab (Figure S1). In the first step, cysteine positional variants with more than 90% of monomer content were selected using nonreducing SDS-PAGE analysis. Further, cysteine positional variants with thiol activity over 1.0 (theoretical value for cystein variant) were selected using a 4,4′-dithiodipyridine (4-PDS) assay. Finally, the criteria for confirming the reaction capacity of selected cysteine positions was set to more than 50% of PEGylation efficiency with 20 kDa PEG-maleimide.

Identification of Cysteine Positions with High Thiol Reactivity. All of the selected variants (26 positions) were expressed, purified by immobilized-metal affinity chromatography, and then analyzed using nonreducing SDS-PAGE (Figure 1A). A band at around 52 kDa was detected in the Tra-Fab-WT, which corresponds to the monomer, while some variants containing the Tra-Fab-Hc-L128C showed various forms. As in the case of the Tra-Fab-Hc-L182C variant, we found a band at around the 76 kDa protein marker, which could correspond to the molecular weight of a Fab-dimer formed due to the intermolecular disulfide bond formation. Thus, considering these results, 24 variants (Hc: 10 variants, Lc: 14 variants) that showed more than 90% of monomer content, such as Tra-Fab-Hc-A140C, were selected for the study. We checked the thiol reactivity of these variants using 4-PDS assay, as summarized in Table 1. Tra-WT (theoretical value: 0) showed 0.36, which was a little higher than expected. In consideration of this basic value, the positions with thiol reactivity greater than 1.0 (theoretical value for cystein variant) were set as criteria and found with a relatively higher rate (14 among 24 positions). The selected variants were conjugated with linear 20 kDa PEG-maleimide and confirmed using nonreducing SDS-PAGE, where the bands around 102 kDa correspond to the PEGylated Fab regions (Figure 1B). We finally selected three positional variants (Hc-A140C in CH1, Lc-Q124C and Lc-L201C in Cκ), which showed over 50% PEGylation efficiency. On the other hand, many variants, such as Tra-Fab-Hc-A141, showed a very low amount or no PEGylated products. As compared to Lc-L201C, the Lc-G200C and Lc-S202C variants, which are located next to the Lc-L201C variant exhibited higher ASA values (43.2% and 114%) and lower thiol reactivities (0.67 and 0.40).

Stable Thiol Reactivity of Selected Cysteine Positional Variants. Periplasmic extraction and Protein-G affinity chromatography were mainly used for preparing the Fab obtained from *E. coli*.[18] We confirmed the thiol reactivity of the four selected clones (Tra-Fab-WT, -Hc-A140C, -Lc-Q124C,

DOI: 10.1021/acs.bioconjchem.5b00080
Bioconjugate Chem. 2015, 26, 1032−1040

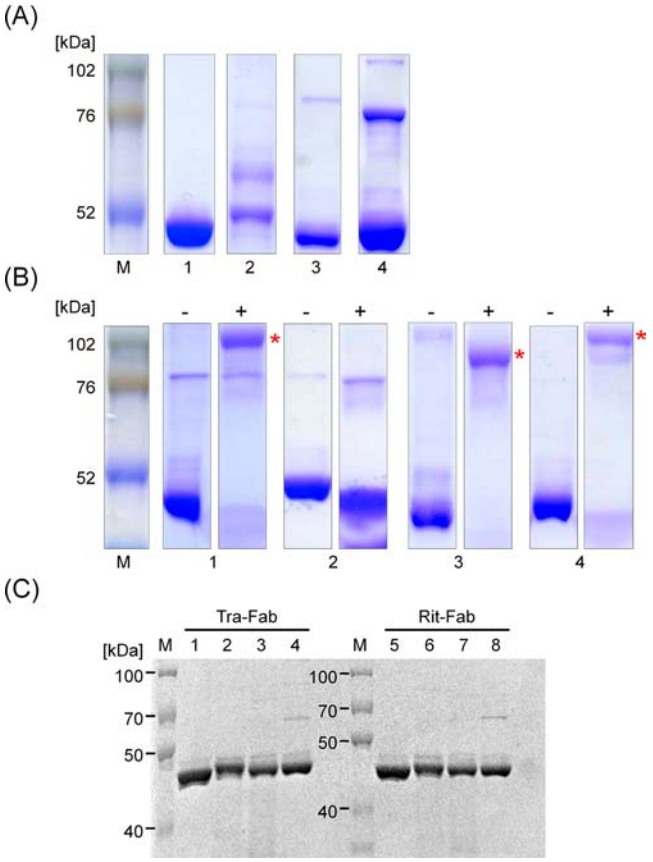

Figure 1. Nonreducing SDS-PAGE analysis of cysteine positional variants. (A) Representative nonreducing SDS-PAGE gels of the purified Tra-Fabs. Lane M: protein standards. Lanes 1−4: Tra-WT, Tra-Hc-L128C, -Hc-A140C, and -Hc-L182C. Monomer Tra-Fab appeared around the 52 kDa protein marker band. (B) PEGylation analysis using nonreducing SDS-PAGE. Lane M: protein standards. Lanes 1−4: Tra-Hc-A140C, -Hc-A141C, -Lc-Q124C, and -Lc-L201C. Left and right gels in each lane show Tra-Fab without or with linear 20 kDa PEG-maleimide. The bands indicated by an asterisk correspond to PEGylated Tra-Fab. (C) Selected cysteine positional variants of Tra-Fab and Rit-Fab. Lane M: protein standards. Lanes 1−4: Tra-Fab-WT, -Hc-A140C, -Lc-Q124C, and -Lc-L201C. Lanes 5−8: Rit-Fab-WT, -Hc-A140C, -Lc-Q124C, and -Lc-L201C. Monomer Fab appeared around the 50 kDa protein marker band.

and -Lc-L201C) using this standard purification process. These clones showed over 90% of monomer content in the nonreducing SDS-PAGE (Figure 1C). From the result of 4-PDS assay, Tra-Fab-WT exhibited 0.17, on the other hand, Tra-Fab-Hc-A140C, -Lc-Q124C, and -Lc-L201C exhibited 1.1, 1.3, and 1.1 (Table 2). These reactivity values were comparable to those purified by TALON. Furthermore, Rit-Fab was selected as an alternative, and we confirmed that Rit-Fab-Hc-A140C, -Lc-Q124C, and -Lc-L201C exhibited more than 90% monomer content (Figure 1C) and thiol reactivity of more than 1.0 (Table 2), as in the case of Tra-Fab.

Physical Properties of Selected Cysteine Positional Variants. Size exclusion chromatography (SEC)-HPLC is routinely used to determine the percentage of monomer of a protein present in aqueous conditions. We confirmed that the three cysteine positional variants (Tra-Fab-Hc-A140C, -Lc-Q124C, and -Lc-L201C) existed mainly as monomers (Figure 2A). We tested the thermal stability of the Tra-Fab-WT, -Hc-A140C-, -Lc-Q124C, and -Lc-L201C mutants using differential

Table 1. ASA Values and Thiol Reactivities[a] of Selected Tra-Fabs

light chain			heavy chain		
variant	ASA (%)	thiol reactivity	variant	ASA (%)	thiol reactivity
WT		0.36			
I117C	5.9	0.81	V125C	3.9	0.65
Q124C	1.1	1.3	L128C	2.2	N/A
A130C	0	1.0	A129C	8.2	1.2
S131C	0.9	1.3	A140C	11.8	1.17
N137C	3.4	1.3	A141C	3.6	1.3
V150C	1.3	1.1	K147C	5.3	1.4
S162C	11.9	0.96	V154C	10.4	0.78
L175C	2.2	0.89	V156C	11.1	0.87
S176C	6.0	0.55	L182C	9.3	N/A
S177C	0	1.1	S183C	4.3	1.0
T178C	14.4	0.35	V188C	7.8	0.95
L181C	10.4	0.77	S192C	11.9	1.0
H198C	7.7	1.1			
G200C	43.2	0.67			
L201C	13.7	1.2			
S202C	114	0.40			

[a]Thiol reactivity was determined by a 4-PDS assay. All the values of thiol reactivity represent the mean of two experiments. N/A denotes not available.

Table 2. Thiol Reactivities[a] of Tra-Fab and Rit-Fab with Selected Cysteine Positions

residue	Tra-Fab	Rit-Fab
WT	0.17 ± 0.034	0.29 ± 0.19
Hc-A140C	1.1 ± 0.07	1.3 ± 0.08
Lc-Q124C	1.3 ± 0.01	1.5 ± 0.05
Lc-L201C	1.1 ± 0.02	1.3 ± 0.03

[a]Thiol reactivities of Tra-Fab and Rit-Fab were determined by three independent assays. The values provided in the table are averages of three independent determinations with standard deviations.

scanning calorimetry, as shown in Figure 2B. The T_m value for Tra-WT was 82.4 °C, which was comparable to the value reported by Kelley et al.[19] These three cysteine positional variants showed similar stability toward thermal denaturation when compared to Tra-WT (Hc-A140C, 82.2 °C; Lc-Q124C, 82.0 °C; and Lc-L201C, 81.8 °C). To determine the dissociation constant (K_D) and the association (k_a) and dissociation rate constants (k_d), CM5 sensor chips were prepared by immobilizing each sample using anti-penta-His antibody. The sensorgrams of selected clones are shown in Figure S2, and further, the K_D values for each clone were determined (Table 3). The binding affinity did not change among the cysteine positional variants, which was also confirmed using ELISA (Figure S3).

Site-Specific PEGylation with Branched PEG (20 kDa ×2)-Maleimide. Cimzia (Certolizumab pegol) is an anti-TNFα PEGylated Fab' obtained via the site-specific attachment of a branched PEG (20 kDa ×2) moiety.[20] The addition of 40 kDa PEG to Fab confers a serum half-life similar to that of an IgG.[21] To investigate the PEGylation efficiency and the effect on binding affinity, Tra-Fab-Hc-A140C, -Lc-Q124C, and -Lc-L201C variants were modified with branched PEG (20 kDa ×2)-maleimide. The bands obtained between 140 and 260 kDa corresponded to the PEGylated Fab in the nonreducing SDS-PAGE (Figure 2C). All three variants showed over 50%

DOI: 10.1021/acs.bioconjchem.5b00080
Bioconjugate Chem. 2015, 26, 1032−1040

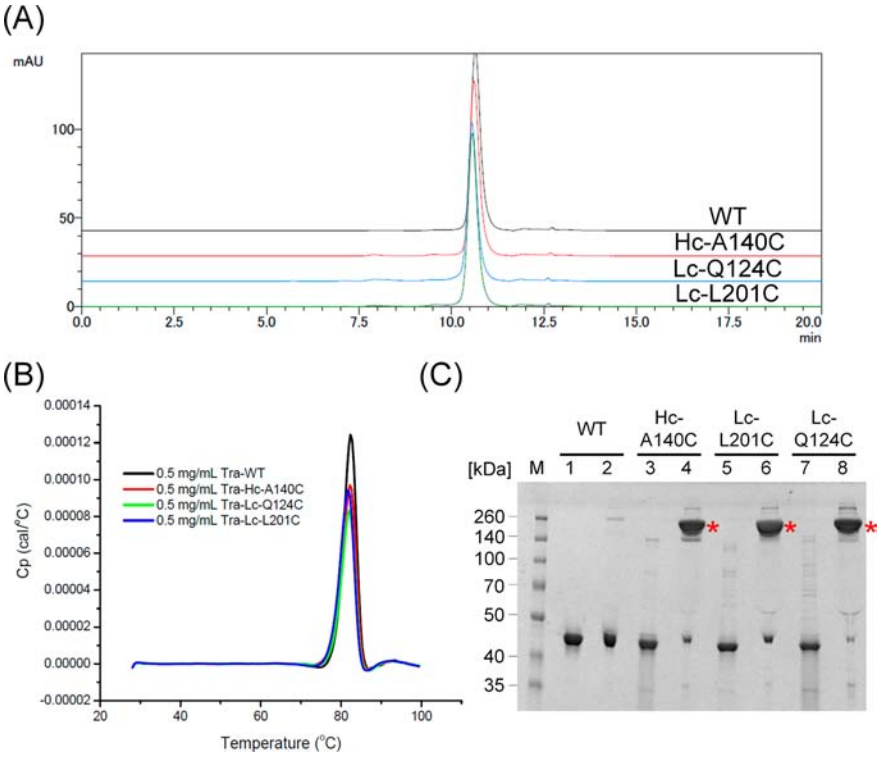

Figure 2. Physical characteristics of selected cysteine positional variants. (A) SEC chromatograms of Tra-Fab-WT, -Hc-A140C, -Lc-Q124C, and -Lc-L201C. Monomer Tra-Fab eluted at 10.6 min. (B) Thermal stability of Tra-Fab-WT, -Hc-A140C, -Lc-Q124C, and -Lc-L201C at a concentration of 0.5 mg/mL in reaction buffer. (C) Nonreducing SDS-PAGE analysis of PEGylated Tra-Fabs. Lane M: protein standards. Lanes 1 and 2: Tra-Fab-WT. Lanes 3 and 4: Tra-Fab-Hc-A140C. Lanes 5 and 6: Tra-Fab-Lc-L201C. Lanes 7 and 8: Tra-Fab-Lc-Q124C. Left (lanes 1, 3, 5, and 7) and right (lanes 2, 4, 6, and 8) gels in each variant show Tra-Fab without or with branched PEG (20 kDa ×2)-maleimide. The bands indicated with an asterisk correspond to PEGylated Tra-Fab.

Table 3. Binding Kinetics of Tra-Fabs and PEGylated Tra-Fabs[a]

sample	k_a ($\times 10^4$) M^{-1} s^{-1}	k_d ($\times 10^{-4}$) s^{-1}	K_D (k_d/k_a) nM
Tra-Fab-WT	7.86	4.90	6.24
Tra-Fab-Hc-A140C	7.83	4.84	6.18
Tra-Fab-Lc-Q124C	7.62	4.68	6.13
Tra-Fab-Lc-L201C	7.89	4.74	6.02
Tra-Hc-A140C-PEG	28.9	4.02	1.39
Tra-Lc-Q124C-PEG	15.7	4.33	2.76
Tra-Lc-L201C-PEG	31.3	3.81	1.22

[a]Presented values refer to the kinetic Biacore measurements shown in Figures S2 and S5. These data are representative of two independent experiments for each sample.

PEGylation efficiency, as in the case of linear 20 kDa PEG-maleimide in nonreducing SDS-PAGE, while comparatively reduced PEGylation was observed for Tra-Fab-WT. We further analyzed the reaction samples using SEC-HPLC (Figure S4) and calculated the PEGylation efficiency as shown in Table 4.

Table 4. PEGylation Efficiency[a] **(%) of Selected Cysteine Positional Variants**

Tra-Fab-WT	Tra-Fab-Hc-A140C	Tra-Fab-Lc-Q124C	Tra-Fab-Lc-L201C
5.8 ± 0.49	88 ± 0.3	94 ± 0.6	83 ± 0.4

[a]PEGylation efficiency was determined by using SEC-HPLC. Values are averages of three independent determinations with standard deviations.

All three variants exhibited over 80% of PEGylation efficiency, with the Tra-Fab-Lc-Q124C variant showing more than 90% efficiency. We prepared each PEGylated Fab sample and evaluated its binding affinity. Figure S5 shows the sensorgrams for Tra-Fab-WT, Tra-Fab-Hc-A140C-PEG, -Lc-Q124C-PEG, and -Lc-L201C-PEG, respectively. The calculated kinetic parameters by Biacore are summarized in Table 3. All three PEGylated Fabs displayed nearly equivalent k_d values, which were about the same as that of the non-PEGylated Tra-Fab. In contrast, we observed that k_a values for the PEGylated Fabs varied in the Biacore analysis depending on the position of the mutation, and hence, the K_D values for PEGylated Fabs decreased 2- to 5-fold compared to the non-PEGylated Tra-Fab. On the other hand, no significant differences in the antigen binding affinity were observed in ELISA among the PEGylated products (Figure S6).

Cytotoxicity of Tra-Fab-MMAE Conjugates. There are two major groups of tubulin inhibitors that have been developed for ADCs: auristatins and maytansine derivatives.[2] Auristatin derivative, maleimidocaproyl-Val-Cit-monomethyl auristatin E (vcMMAE), has been designed for linking to cysteine residues via maleimide. We prepared Tra-Fab-vcMMAE conjugates via selected cysteine positions. The formations of Tra-Fab-Hc-A140C-MMAE, -Lc-Q124C-MMAE, and -Lc-L201C-MMAE were confirmed using LC-MS analysis (Figure S7). Tra-Fab-Lc-Q124C-MMAE conjugates exerted potential in vitro cytotoxicity against Her2-amplified breast cancer cell line SK-BR-3, and showed minimal antiproliferative activity for the breast cancer cell line MCF-7, expressing normal levels in the concentration range tested

DOI: 10.1021/acs.bioconjchem.5b00080
Bioconjugate Chem. 2015, 26, 1032−1040

(Figure 3A,B). Her2-depdendent cytotoxicity was also confirmed using a competition assay with excess free Tra-Fab-WT

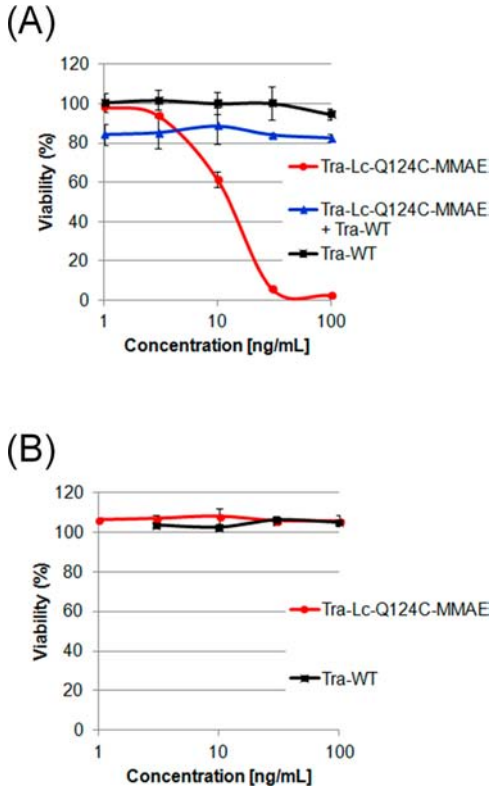

Figure 3. In vitro cytotoxicity of Tra-Fab-Lc-Q124C-MMAE. (A) Potent cytotoxicity was observed in SK-BR-3 with high levels of Her2 protein. (B) No antiproliferative effect was observed in MCF-7 with normal/low levels of Her2 protein.

(Figure 3A). Tra-Fab-Hc-A140C-MMAE and -Lc-L201C-MMAE conjugates also showed similar cytotoxicity against the SK-BR-3 cell line (Figure S8).

DISCUSSION

In this study, we successfully found three original cysteine positions in the Fab fragment (CH1, Hc-A140C; and Cκ, Lc-Q124C and Lc-L201C), which were located at relatively less exposed positions and had less than 20% of ASA. In particular, the Lc-Q124C variant showed the highest thiol reactivity in spite of having the lowest ASA value of less than 5%. The Lc-G200C and Lc-S202C positional variants located near the Lc-L201C mutation showed a higher ASA, but lower thiol reactivity compared to the Lc-L201C variant. In addition, Hc-A141C that is located next to Hc-A140C position produced no PEGylated product. For extended conformations of polypeptide chains, residue side chains naturally alternate their direction from one sequence position to the next, so it is to be expected that adjacent residues on the surface of a three-dimensional structure will exhibit behavior that alternates accordingly. In consideration of these findings, the conjugation efficiency of engineered cysteine residues was determined not by the structural region, but by the positions themselves. We intensively searched for these cysteine positions in the Fab constant region for the following reasons. First, the Fab fragment can be easily expressed in *E. coli*. This is suitable for evaluating many cysteine positional variants because of the rapid growth of bacterial cells, a requirement for simple and inexpensive media, and an appropriate fermentation technology. Second, these cysteine positions in the Fab constant region have a very low effect on the antigen-binding activity of the antibody and could be applied to a number of clones. In fact, the cysteine variants of Tra-Fab exhibited similar binding affinity as that observed for Tra-Fab-WT, and further the thiol reactivity was observed to be unchanged between the Tra-Fab and Rit-Fab. Third, the effector functions such as antibody-dependent cell-mediated cytotoxicity mediated by the Fc region would not be affected by the introduction of these cysteine mutations in the Fab constant region. Finally, these cysteine positional mutations could also be applied to other molecules such as IgG, monovalent antibodies,[22] and bispecific antibodies,[23] which contain the Fab region. Recently, aglycosylated full-length IgG antibodies have been shown to be produced in the *E. coli* periplasmic fraction, as in the case of Fab expression.[24] The cysteine positions found in the Fab fragment on the phage surface were applied to IgG antibodies (THIOMAB) that were produced in Chinese hamster ovary (CHO) cells.[8] In consideration of these facts, the selected engineered cysteine residues could be used for the design of recombinant IgG forms.

Nonreducing SDS-PAGE and SEC-HPLC analysis showed that Tra-Fab-Hc-A140C, -Lc-Q124C, and -Lc-L201C existed mainly as monomers. In addition, these cysteine variants showed similar thermal stability in comparison to Tra-WT, which indicates that the selected cysteine positions do not disturb the structurally important interactions. These findings suggest that our selected cysteine positions had no effect on the physical characteristics of the Fab region, although these mutations were located at structurally buried positions. On the other hand, some cysteine variants such as Tra-Fab-Hc-L128C exhibited several bands on the nonreducing SDS-PAGE gel, indicating that denaturation was induced due to substitution by cysteine residues. The dimer content in the engineered cysteine variants varied depending on the cysteine positions. Considering these results, our strategy for evaluating the conjugation efficiency of recombinant Fab was useful for examining the physical features of the cysteine positional variants and for elucidating these original cysteine positions; however, these selection schemes required labor-intensive and time-consuming efforts.

PEGylation is an attractive strategy used to enhance the therapeutic efficacy of proteins with a short serum half-life.[25] The obvious trend applied in the development of the PEGylated therapeutic proteins is a shift from random to site-specific PEGylation reactions, resulting in homogeneous products.[26] In the case of the production of PEGylated-Fab' Cimzia, reductive activation of the hinge region cysteine residues, under mild reducing conditions, was required prior to PEGylation.[21] Disulfide-bridged PEGylation selectively alkylates both the sulfur atoms derived from a native disulfide bond; however, a reductive process prior to PEGylation was also required.[27] In general, thiol PEGylation of cysteine residues enclosed in less solvent-accessible hydrophobic patches is difficult to achieve. Veronese et al. reported a negligible degree of PEGylation for Cys17 on granulocyte-colony stimulating factor when PEGylation was carried out under physiological conditions, whereas successful coupling was obtained under transient denaturing conditions.[17] By contrast, our selected cysteine positional variants could be efficiently PEGylated in

DOI: 10.1021/acs.bioconjchem.5b00080
Bioconjugate Chem. 2015, 26, 1032−1040

the absence of any reductive or denaturing conditions, in spite of their lower solvent accessibility.

We observed an unexpected 2- to 4-fold increment in the k_a values for PEGylated-Tra-Fabs in comparison to that for the Tra-Fab-WT, while k_d values were unchanged in Biacore analysis. On the other hand, similar binding curves were observed for the PEGylated Tra-Fabs in ELISA. Thus, these results together suggest that PEGylation in the Fab constant region has no significant effect on the binding affinity. However, PEGylation in C-turminal of Fab could result in decreased k_a value under the experimental condition of immobilized antigen and PEGylated Fab in the mobile phase.[27] Hence, further structure-based study is needed to clarify the positional effect of PEGylation on the binding affinity.

MMAE is one of the validated payloads as proved by the FDA approval of Adcetris (anti-CD30 chimeric antibody−MMAE conjugate).[28] All of the Tra-Fab-MMAE conjugates exerted potent in vitro cytotoxicity on the SK-BR-3 cell line. In addition, the LC-MS analysis mainly showed conjugated forms, suggesting that a higher conjugation efficiency was observed with MMAE without any pretreatment. Our results suggest that the selected cysteine positional variants could easily produce site-specific antibody−drug conjugates, although further studies on the application of IgG format would be required. In consideration of the binding capacity observed for our cysteine positional variants toward the macromolecules such as PEG, in the future, functional macromolecules such as peptides and nucleotides could also be easily conjugated with these variants.

Serum albumin is one of the known native proteins that has a single unpaired cysteine residue, similar to our cysteine positional variants.[29] The single thiol group present in human serum albumin (HSA), Cys34 is the most abundant thiol group in the plasma. Cys34 forms mixed disulfides with low-molecular-weight thiols; however, it is mainly present in the reduced form (75%).[30] In addition, purified serum albumin could be conjugated with various-sized molecules through Cys34.[31,32] We calculated the ASA value for Cys34 based on the structural information on HSA (PDB: 1AO6), using the same procedure as used in the case of Tra-Fab. It is interesting to note that the ASA value of Cys34 was found to be low (0.7%), which is similar to those of our selected cysteine positions. The crystal structure of HSA[29] suggests that Cys34 is located on the surface of domain I; however, the sulfur atom is oriented toward the interior of the protein and is surrounded by the side chains of the Pro35, His39, Val77, and Tyr84 residues, resulting in a lower ASA value. These findings suggest that the orientation of the side chain, in addition to the position of engineered cysteine residues, could be responsible for the thiol reactivity and higher binding capacity of these variants for various-sized molecules. Further structural analysis of our cysteine positional variants would enable finding rational substitutes for cysteine with high thiol reactivity.

To our knowledge, very few reports are available on engineered cysteine residues present on the less exposed positions in proteins, including antibodies. We found the original three cysteine residues present at less exposed positions, which have never been explored previously. We could produce site-specific Fab conjugates with various-sized molecules (from small molecules such as MMAE to high-molecular-weight PEG) through these cysteine positions. In addition, cysteine mutations at our selected positions had no effect on the thermal stability, monomer content, and binding affinity. In conclusion, our selected cysteine positions in the Fab constant region could provide an alternative approach for site-specific antibody−drug conjugation. Furthermore, our concept for introducing cysteine residues at less exposed positions on the protein could be applied to other proteins for site-specific conjugation via engineered cysteines.

EXPERIMENTAL PROCEDURES

Materials. 4-PDS was obtained from Nacalai Tesque (Kyoto, Japan). Linear 20 kDa PEG-maleimide (SUNBRIGHT ME-200 MAOB) and branched PEG (20 kDa ×2)-maleimide (SUNBRIGHT GL2-400MA3) were purchased from NOF.-CORPORATION (Tokyo, Japan). The murine anti-penta-His antibody was obtained from QIAGEN (Hilden, Germany), and the HRP-conjugate was prepared using the Peroxidase Labeling Kit-NH_2 (DOJINDO, Kumamoto, Japan). vcMMAE was purchased from MedChem Express (Monmouth Junction, NJ). Her2-GST and Her2-flag fusion proteins were made and validated in-house. The reaction buffer used was composed of 20 mM sodium citrate (pH 6.0) and 150 mM NaCl. Breast carcinoma cell lines (SKBR-3 and MCF7) and the *E. coli* strain W3110 were obtained from American Type Culture Collection (Manassas, VA).

Vector Design for Fab Expression. The plasmid, pFLAG-CTS-Fab (Figure S9), was designed to coexpress the light and heavy chain of the Fab fragment, which was cloned between the *Nde*I and *Sal*I sites on pFLAG-CTS (Sigma-Aldrich, St. Louis, MO). The operon was under the transcriptional control of the tac promoter (P*tac*), which is inducible by isopropyl-β-D-thiogalactopyranoside (IPTG).[33] Each Fab chain was preceded by a PelB signal sequence to direct the secretion into the periplasmic space of *E. coli*.[34] In order to be used for detection and affinity purification, the hexa-histidine tag sequence was added to the C-terminal of the heavy chain. The genes of the CH1 heavy chain constant region and Cκ light chain constant region were each connected to the genes encoding identical amino acid sequences of variable regions of therapeutic anti-ErbB2 antibody trastuzumab[35] (Tra-Fab) and anti-CD20 antibody rituximab[36] (Rit-Fab). The codons for selected positions in human Cκ (defined by Kabat number) or human CH1 (defined by EU number) constant regions were changed to cysteine using PCR.

ASA. The ASA was calculated using the DSSP program[37] based on the structural information in the Protein Data Bank for Tra-Fab (PDB: 1FVD),[38] assuming that the cysteine positional mutant has exactly the same static structure as the pdb entry. To determine the percentage values, the ASA value of amino acid 'X' of the Ala-X-Ala tripeptide was assigned to a value of 1.0.

Fab Expression. Fab was expressed in *E. coli* strain W3110 transformed with plasmid pFLAG-CTS-Fab. Single colonies were grown overnight at 37 °C in 10 mL of LB medium containing 100 μg/mL of ampicillin. Overnight cultures were diluted to 200 mL of Super Broth and incubated at 37 °C until an OD_{600} of 2.0 was obtained, and further incubated at 22 °C overnight with the addition of 1 mM IPTG. The cells were pelleted at 5000 rpm and frozen at −80 °C.

Immobilized-Metal Affinity Chromatography. Frozen cells were resuspended in 20 mL of B-PER Bacterial Protein Extraction Reagent (Thermo Fisher Scientifec, Waltham, MA), shaken at room temperature for 10 min, and centrifuged at 7000 rpm for 25 min. The supernatant was applied to a 1 mL TALON Metal Affinity Resin (Clontech, Mountain View, CA)

DOI: 10.1021/acs.bioconjchem.5b00080
Bioconjugate Chem. 2015, 26, 1032−1040

and washed with 10 mL of 50 mM sodium phosphate (pH 6.7) and 300 mM NaCl solution. The bound Fab was eluted with 1.5 mL of 50 mM sodium phosphate, 300 mM NaCl, and 150 mM imidazole buffer. The buffer exchange into reaction buffer was accomplished using the Amicon Ultra-0.5 device (Merck Millipore, Billerica, MA).

Protein G Affinity Chromatography. Frozen cells were resuspended in 15 mL of reaction buffer, incubated at 60 °C for 15 min, and centrifuged at 7000 rpm for 15 min. The supernatant was applied to a 1 mL Prosep-G Resin (Merck Millipore) and washed with 10 mL of reaction buffer. The bound Fab was eluted with 2 mL of 10 mM sodium citrate (pH 3.0), and neutralized using 1 M Tris-HCl (pH 8.0). The buffer exchange into reaction buffer was accomplished using the Amicon Ultra-0.5 device (Merck Millipore).

Thiol Reactivity Analysis by 4-PDS. 4-PDS reacts with the thiol groups under weak acidic conditions to form 4-mercaptopyridine with an absorbance at 324 nm.[39] Purified Fabs were mixed with the reaction buffer, containing 4-PDS, such that the final solution contained 10 μM Fab and 500 μM of 4-PDS. A standard curve was derived from the titration of N-acetyl-L-cysteine with 4-PDS. The reaction for 30 min at room temperature was followed by monitoring the absorption at 324 nm. Thiol reactivity was calculated as the ratio of measured value and theoretical value at 10 μM of N-acetyl-L-cysteine, obtained from the standard curve. Theoretically, thiol reactivity of a molecule with one free thiol is 1.0.

PEGylation with the Linear 20 kDa PEG-maleimide. A solution of 10 μM Tra-Fab was mixed with a 20-fold molar excess of linear 20 kDa PEG-maleimide for 2 h at room temperature in the reaction buffer. Approximately 100 pmol of reaction mixtures were analyzed using nonreducing SDS-PAGE. After staining of the gel using Coomassie Blue, protein bands were visualized using the densitometer. PEGylation efficiencies were calculated by the comparison of the band densities of each molecular species.

SEC. SEC was performed using Prominence (SHIMADZU, Kyoto, Japan). Approximately 200 pmol samples were injected into the TSKgel G3000SW$_{XL}$ columns (TOSOH, Tokyo, Japan). The mobile phase was the reaction buffer. The flow rate was 1 mL/min for 30 min. Detection was conducted by recording absorbance at 280 nm.

Differential Scanning Calorimetry. Thermal denaturation experiments were performed on a MicroCal VP-Capillary differential scanning calorimeter (GE Healthcare, Little Chalfont, United Kingdom). Fab solutions were adjusted to 0.5 mg/mL in reaction buffer and heated to 100 °C in the calorimeter using a heating rate of 60 °C/min. The observed melting curves were baseline-substituted and normalized using the software supplied by the manufacturer.

Binding Analysis by ELISA. The 96-well ELISA plate was coated with Her2-GST fusion protein (1 μg/mL) and kept overnight at 4 °C. After washing three times with TBST (TBS and 0.05% Tween-20), 150 μL of 1% BSA in PBS was added to each well and incubated for 1 h at room temperature. The wells were further washed three times with TBST. Samples were prepared in the reaction buffer at a range of concentrations, added (50 μL) to each well, and then incubated for 1 h at room temperature. The wells were then washed three times with TBST followed by incubation with 50 μL of anti-penta-His antibody HRP conjugate (diluted 1000 or 5000 times in 1% BSA) for 1 h at room temperature. The wells were again washed three times with TBST, developed using 50 μL of TMB for approximately 5 min, and quenched by addition of 50 μL of 0.5 N H_2SO_4. The absorbance was read using a ARVO X3 (PerkinElmer, Waltham, MA) at 450 nm.

Binding Analysis by Biacore. Binding affinity and kinetics analyses were conducted using the Biacore T100 (GE Healthcare). To circumvent errors from different sample concentrations, Tra-Fab or PEGylated-Tra-Fab was immobilized, then a range of concentrations of Her2-flag were passed as following procedures. The murine anti-penta-His antibody, diluted at 30 μg/mL in 10 mM sodium acetate (pH 5.0), was immobilized on a CM5 sensor chip for 600 s at a flow rate of 10 μL/min via amine coupling. Further, 5 nM Tra-Fab or 250 nM Tra-Fab-PEG in HBS-EP+ running buffer (10 mM HEPES, pH 7.4, 150 mM NaCl, 3 mM EDTA, 0.005% surfactant P20) were captured for 45 s at a flow rate of 10 μL/min. A range of concentrations of Her2-flag (0, 0.34, 1.03, 3.09, 9.26, 27.7, 83.3, and 250 nM) in HBS-EP+ running buffer were passed over the immobilized Tra-Fab or Tra-Fab-PEG for 180 s at a flow rate of 30 μL/min during the association phase. At the dissociation phases, HBS-EP+ running buffer was exposed for 600 s at a flow rate of 30 μL/min. Chip regeneration was accomplished by exposure to 10 mM Gly-HCl (pH 3.0), 1 M magnesium chloride for 20 s at a flow rate of 10 μL/min. All kinetic measurements were conducted at 25 °C. Binding kinetic parameters, including the k_a, k_d, and K_D values, were calculated using Biacore evaluation software.

PEGylated Fab with the Branched PEG (20 kDa ×2)-maleimide. A solution of 50 μM Tra-Fab was mixed with a 10-fold molar excess of branched PEG (20 kDa ×2)-maleimide and kept overnight at 4 °C. PEGylation efficiencies were calculated by the comparison of the relative area under the peaks obtained for each molecular species in SEC-HPLC. Purification of PEGylated Fab was carried out while monitoring the absorption value at 280 nm using ÄKTA purifier (GE Healthcare) under the following column conditions: Superose 12 10/300GL (GE Healthcare); eluent, reaction buffer; flow rate, 0.5 mL/min; and temperature, 4 °C.

Preparation of Tra-Fab-vcMMAE Conjugates. Tra-Fabs, obtained after Protein G purification, were further purified on a cation exchange column (Mono S 5/50 GL, GE Healthcare) with mobile phase A, 20 mM sodium citrate pH 6.0; and mobile phase B. 1 M NaCl and 20 mM sodium citrate pH 6.0. A linear gradient of 0−100% B was used to remove the endotoxin from the samples. The buffer exchange into reaction buffer was accomplished using the Amicon Ultra-0.5 device (Merck Millipore). Tra-Fab was then conjugated with a 10-fold molar excess of vcMMAE in the reaction buffer, including 20% acetonitrile, overnight at 4 °C. Further, the removal of the free vcMMAE and buffer exchange into reaction buffer were accomplished using the Amicon Ultra-0.5 device (Merck Millipore). Formation of the Tra-Fab-MMAE conjugate was evaluated using LC-MS analysis as described below.

Mass Spectrometric Analysis. All experiments were performed on a Waters Synapt high-definition mass spectrometer fitted with an atmospheric pressure ionization electrospray source (Waters Corporation, Milford, MA) and coupled with an ACQUITY UPLC BEH200 SEC (Waters Corporation). The sample separation was conducted under isocratic conditions at a flow rate of 0.2 mL/min. The mobile phase was acetonitrile:water (30:70) with 0.1% formic acid and 0.1% trifluoroacetic acid. A positive time-of-flight MS scan was acquired. Data collection and processing were controlled by *MassLynx 4.1* software.

DOI: 10.1021/acs.bioconjchem.5b00080
Bioconjugate Chem. 2015, 26, 1032−1040

In Vitro Cytotoxicity. On the day of plating, 3000 cells/well were seeded onto the 96 well plates and the cells were allowed to attach to the plate overnight at 37 °C in a humidified atmosphere of 5% CO_2. A serial dilution of wild-type Tra-Fab and Tra-Fab-MMAE conjugates were added and the cells were incubated for 120 h at 37 °C. The same procedure with excess amount of Tra-WT (10 μg/mL) was used as a competitive inhibition assay. Cell Titer-Glo Luminescent Cell Viability Assay (Promega, Madison, MA) reagent was added to the wells for 10 min at room temperature and the luminescent signal was measured by the ARVO X3 system (PerkinElmer).

■ ASSOCIATED CONTENT

Ⓢ Supporting Information

Selected cysteine positions highlighted onto Tra-Fab structure, sensorgrams of Tra-Fabs, superimposed ELISA binding curves of Tra-Fabs, SEC chromatograms of PEGylated Tra-Fabs, sensorgrams of PEGylated Tra-Fabs, ELISA binding curves of PEGylated Tra-Fabs, deconvoluted masses of Tra-Fab-MMAE conjugates, cytotoxicity of Tra-Fab-Hc-A140C-MMAE and -Lc-L20C-MMAE conjugates, and schematic view of Fab expression vector. The Supporting Information is available free of charge on the ACS Publications website at DOI: 10.1021/acs.bioconjchem.5b00080.

■ AUTHOR INFORMATION

Corresponding Author

*E-mail: yasuhisa.shiraishi@kyowa-kirin.co.jp. Phone: +81-42-725-2555. Fax: +81-42-726-9790.

Notes

The authors declare no competing financial interest.

■ ACKNOWLEDGMENTS

The authors thank Eri Suzuki-Takanami and Yoshiko Ishikawa-Matsumoto for their technical assistance with the LC-MS instrument.

■ ABBREVIATIONS

ADC, antibody−drug conjugate; ASA, accessible surface area; DAR, drug-to-antibody ratio; Tra, trastuzumab; Rit, rituximab; 4-PDS, 4,4′-dithiodipyridine; and SEC, size exclusion chromatography

■ REFERENCES

(1) Mullard, A. (2013) Maturing antibody-drug conjugate pipeline hits 30. *Nat. Rev. Drug Discovery 12*, 329−32.

(2) Chari, R. V., Miller, M. L., and Widdison, W. C. (2014) Antibody-drug conjugates: an emerging concept in cancer therapy. *Angew. Chem., Int. Ed. 53*, 3796−827.

(3) Wang, L., Amphlett, G., Blattler, W. A., Lambert, J. M., and Zhang, W. (2005) Structural characterization of the maytansinoid-monoclonal antibody immunoconjugate, huN901-DM1, by mass spectrometry. *Protein Sci. 14*, 2436−46.

(4) Hamblett, K. J., Senter, P. D., Chace, D. F., Sun, M. M., Lenox, J., Cerveny, C. G., Kissler, K. M., Bernhardt, S. X., Kopcha, A. K., Zabinski, R. F., et al. (2004) Effects of drug loading on the antitumor activity of a monoclonal antibody drug conjugate. *Clin. Cancer Res. 10*, 7063−70.

(5) Behrens, C. R., and Liu, B. (2014) Methods for site-specific drug conjugation to antibodies. *MAbs 6*, 46−53.

(6) Panowksi, S., Bhakta, S., Raab, H., Polakis, P., and Junutula, J. R. (2014) Site-specific antibody drug conjugates for cancer therapy. *MAbs 6*, 34−45.

(7) Junutula, J. R., Bhakta, S., Raab, H., Ervin, K. E., Eigenbrot, C., Vandlen, R., Scheller, R. H., and Lowman, H. B. (2008) Rapid identification of reactive cysteine residues for site-specific labeling of antibody-Fabs. *J. Immunol. Methods 332*, 41−52.

(8) Junutula, J. R., Raab, H., Clark, S., Bhakta, S., Leipold, D. D., Weir, S., Chen, Y., Simpson, M., Tsai, S. P., Dennis, M. S., et al. (2008) Site-specific conjugation of a cytotoxic drug to an antibody improves the therapeutic index. *Nat. Biotechnol. 26*, 925−32.

(9) Lyons, A., King, D. J., Owens, R. J., Yarranton, G. T., Millican, A., Whittle, N. R., and Adair, J. R. (1990) Site-specific attachment to recombinant antibodies via introduced surface cysteine residues. *Protein Eng. 3*, 703−8.

(10) Stimmel, J. B., Merrill, B. M., Kuyper, L. F., Moxham, C. P., Hutchins, J. T., Fling, M. E., and Kull, F. C., Jr. (2000) Site-specific conjugation on serine right-arrow cysteine variant monoclonal antibodies. *J. Biol. Chem. 275*, 30445−50.

(11) Voynov, V., Chennamsetty, N., Kayser, V., Wallny, H. J., Helk, B., and Trout, B. L. (2010) Design and application of antibody cysteine variants. *Bioconjugate Chem. 21*, 385−92.

(12) Zimmerman, E. S., Heibeck, T. H., Gill, A., Li, X., Murray, C. J., Madlansacay, M. R., Tran, C., Uter, N. T., Yin, G., Rivers, P. J., et al. (2014) Production of site-specific antibody-drug conjugates using optimized non-natural amino acids in a cell-free expression system. *Bioconjugate Chem. 25*, 351−61.

(13) Tian, F., Lu, Y., Manibusan, A., Sellers, A., Tran, H., Sun, Y., Phuong, T., Barnett, R., Hehli, B., Song, F., et al. (2014) A general approach to site-specific antibody drug conjugates. *Proc. Natl. Acad. Sci. U. S. A. 111*, 1766−71.

(14) Drake, P. M., Albers, A. E., Baker, J., Banas, S., Barfield, R. M., Bhat, A. S., de Hart, G. W., Garofalo, A. W., Holder, P., Jones, L. C., et al. (2014) Aldehyde tag coupled with HIPS chemistry enables the production of ADCs conjugated site-specifically to different antibody regions with distinct in vivo efficacy and PK outcomes. *Bioconjugate Chem. 25*, 1331−41.

(15) Dennler, P., Chiotellis, A., Fischer, E., Bregeon, D., Belmant, C., Gauthier, L., Lhospice, F., Romagne, F., and Schibli, R. (2014) Transglutaminase-based chemo-enzymatic conjugation approach yields homogeneous antibody-drug conjugates. *Bioconjugate Chem. 25*, 569−78.

(16) Woo, H. J., Lotz, M. M., Jung, J. U., and Mercurio, A. M. (1991) Carbohydrate-binding protein 35 (Mac-2), a laminin-binding lectin, forms functional dimers using cysteine 186. *J. Biol. Chem. 266*, 18419−22.

(17) Veronese, F. M., Mero, A., Caboi, F., Sergi, M., Marongiu, C., and Pasut, G. (2007) Site-specific pegylation of G-CSF by reversible denaturation. *Bioconjugate Chem. 18*, 1824−30.

(18) Carter, P., Kelley, R. F., Rodrigues, M. L., Snedecor, B., Covarrubias, M., Velligan, M. D., Wong, W. L., Rowland, A. M., Kotts, C. E., Carver, M. E., et al. (1992) High level Escherichia coli expression and production of a bivalent humanized antibody fragment. *Bio/Technology 10*, 163−7.

(19) Kelley, R. F., O'Connell, M. P., Carter, P., Presta, L., Eigenbrot, C., Covarrubias, M., Snedecor, B., Bourell, J. H., and Vetterlein, D. (1992) Antigen binding thermodynamics and antiproliferative effects of chimeric and humanized anti-p185HER2 antibody Fab fragments. *Biochemistry 31*, 5434−41.

(20) Goel, N., and Stephens, S. (2010) Certolizumab pegol. *MAbs 2*, 137−47.

(21) Humphreys, D. P., Heywood, S. P., Henry, A., Ait-Lhadj, L., Antoniw, P., Palframan, R., Greenslade, K. J., Carrington, B., Reeks, D. G., Bowering, L. C., et al. (2007) Alternative antibody Fab' fragment PEGylation strategies: combination of strong reducing agents, disruption of the interchain disulphide bond and disulphide engineering. *Protein Eng. Des. Sel. 20*, 227−34.

(22) Xiang, H., Bender, B. C., Reyes, A. E., 2nd, Merchant, M., Jumbe, N. L., Romero, M., Davancaze, T., Nijem, I., Mai, E., Young, J., et al. (2013) Onartuzumab (MetMAb): using nonclinical pharmacokinetic and concentration-effect data to support clinical development. *Clin. Cancer Res. 19*, 5068−78.

DOI: 10.1021/acs.bioconjchem.5b00080
Bioconjugate Chem. 2015, 26, 1032−1040

(23) Spiess, C., Merchant, M., Huang, A., Zheng, Z., Yang, N. Y., Peng, J., Ellerman, D., Shatz, W., Reilly, D., Yansura, D. G., et al. (2013) Bispecific antibodies with natural architecture produced by co-culture of bacteria expressing two distinct half-antibodies. *Nat. Biotechnol. 31*, 753−8.
(24) Ju, M. S., and Jung, S. T. (2014) Aglycosylated full-length IgG antibodies: steps toward next-generation immunotherapeutics. *Curr. Opin. Biotechnol. 30C*, 128−139.
(25) Jevsevar, S., Kunstelj, M., and Porekar, V. G. (2010) PEGylation of therapeutic proteins. *Biotechnol. J. 5*, 113−28.
(26) Pfister, D., and Morbidelli, M. (2014) Process for protein PEGylation. *J. Controlled Release 180*, 134−49.
(27) Khalili, H., Godwin, A., Choi, J. W., Lever, R., and Brocchini, S. (2012) Comparative binding of disulfide-bridged PEG-Fabs. *Bioconjugate Chem. 23*, 2262−77.
(28) Katz, J., Janik, J. E., and Younes, A. (2011) Brentuximab Vedotin (SGN-35). *Clin. Cancer Res. 17*, 6428−36.
(29) Sugio, S., Kashima, A., Mochizuki, S., Noda, M., and Kobayashi, K. (1999) Crystal structure of human serum albumin at 2.5 A resolution. *Protein Eng. 12*, 439−46.
(30) Turell, L., Radi, R., and Alvarez, B. (2013) The thiol pool in human plasma: the central contribution of albumin to redox processes. *Free Radic. Biol. Med. 65*, 244−53.
(31) Jiang, Y., Lu, H., Khine, Y. Y., Dag, A., and Stenzel, M. H. (2014) Polyion complex micelle based on albumin-polymer conjugates: multifunctional oligonucleotide transfection vectors for anticancer chemotherapeutics. *Biomacromolecules 15*, 4195−205.
(32) Narazaki, R., Maruyama, T., and Otagiri, M. (1997) Probing the cysteine 34 residue in human serum albumin using fluorescence techniques. *Biochim. Biophys. Acta 1338*, 275−81.
(33) de Boer, H. A., Comstock, L. J., and Vasser, M. (1983) The tac promoter: a functional hybrid derived from the trp and lac promoters. *Proc. Natl. Acad. Sci. U. S. A. 80*, 21−5.
(34) Lei, S. P., Lin, H. C., Wang, S. S., Callaway, J., and Wilcox, G. (1987) Characterization of the Erwinia carotovora pelB gene and its product pectate lyase. *J. Bacteriol. 169*, 4379−83.
(35) Carter, P., Presta, L., Gorman, C. M., Ridgway, J. B., Henner, D., Wong, W. L., Rowland, A. M., Kotts, C., Carver, M. E., and Shepard, H. M. (1992) Humanization of an anti-p185HER2 antibody for human cancer therapy. *Proc. Natl. Acad. Sci. U. S. A. 89*, 4285−9.
(36) Natsume, A., In, M., Takamura, H., Nakagawa, T., Shimizu, Y., Kitajima, K., Wakitani, M., Ohta, S., Satoh, M., Shitara, K., et al. (2008) Engineered antibodies of IgG1/IgG3 mixed isotype with enhanced cytotoxic activities. *Cancer Res. 68*, 3863−72.
(37) Kabsch, W., and Sander, C. (1983) Dictionary of protein secondary structure: pattern recognition of hydrogen-bonded and geometrical features. *Biopolymers 22*, 2577−637.
(38) Eigenbrot, C., Randal, M., Presta, L., Carter, P., and Kossiakoff, A. A. (1993) X-ray structures of the antigen-binding domains from three variants of humanized anti-p185HER2 antibody 4D5 and comparison with molecular modeling. *J. Mol. Biol. 229*, 969−95.
(39) Grassetti, D. R., and Murray, J. F., Jr. (1967) Determination of sulfhydryl groups with 2,2′- or 4,4′-dithiodipyridine. *Arch. Biochem. Biophys. 119*, 41−9.

DOI: 10.1021/acs.bioconjchem.5b00080
Bioconjugate Chem. 2015, 26, 1032−1040